Headline Indicators for Global Climate Monitoring

Blair Trewin, Anny Cazenave, Stephen Howell, Matthias Huss, Kirsten Isensee, Matthew D. Palmer, Oksana Tarasova, Alex Vermeulen

BAMS Article

Headline Indicators for Global Climate Monitoring

Blair Trewin, Anny Cazenave, Stephen Howell, Matthias Huss, Kirsten Isensee, Matthew D. Palmer, Oksana Tarasova, and Alex Vermeulen

ABSTRACT: The World Meteorological Organization has developed a set of headline indicators for global climate monitoring. These seven indicators are a subset of the existing set of essential climate variables (ECVs) established by the Global Climate Observing System and are intended to provide the most essential parameters representing the state of the climate system. These indicators include global mean surface temperature, global ocean heat content, state of ocean acidification, glacier mass balance, Arctic and Antarctic sea ice extent, global CO_2 mole fraction, and global mean sea level. This paper describes how well each of these indicators are currently monitored, including the number and quality of the underlying datasets; the health of those datasets; observation systems used to estimate each indicator; the timeliness of information; and how well recent values can be linked to preindustrial conditions. These aspects vary widely between indicators. While global mean surface temperature is available in close to real time and changes from preindustrial levels can be determined with relatively low uncertainty, this is not the case for many other indicators. Some indicators (e.g., sea ice extent) are largely dependent on satellite data only available in the last 40 years, while some (e.g., ocean acidification) have limited underlying observational bases, and others (e.g., glacial mass balance) with data only available a year or more in arrears.

https://doi.org/10.1175/BAMS-D-19-0196.1
Corresponding author: Blair Trewin, blair.trewin@bom.gov.au
Supplemental material: https://doi.org/10.1175/BAMS-D-19-0196.2
In final form 8 July 2020

AFFILIATIONS: Trewin—Australian Bureau of Meteorology, Melbourne, Victoria, Australia; **Cazenave**—LEGOS, Observatoire Midi-Pyrenees, Toulouse, France; **Howell**—Climate Research Division, Environment and Climate Change Canada, Toronto, Ontario, Canada; **Huss**—Laboratory of Hydraulics, Hydrology and Glaciology (VAW), ETH Zurich, Zurich, and Swiss Federal Institute for Forest, Snow and Landscape Research (WSL), Birmensdorf, Switzerland; **Isensee**—Intergovernmental Oceanographic Commission, UNESCO, Paris, France; **Palmer**—Met Office Hadley Centre, Exeter, United Kingdom; **Tarasova**—World Meteorological Organization, Geneva, Switzerland; **Vermeulen**—Lund University, Lund, Sweden

A wide range of variables is used to monitor the state of the global climate. This monitoring includes reporting on annual time scales, such as through the World Meteorological Organization's (WMO) State of the Climate series (e.g., WMO 2019) and the State of the Climate reports published through *BAMS* (e.g., Blunden et al. 2018), as well through the systematic Assessment Reports of the Intergovernmental Panel on Climate Change (IPCC) (IPCC 2013, 2019a,b).

Key indicators play an important role in many forms of global monitoring. They are quantified, objective, based on data provided by virtually all countries, and used to demonstrate change in the climate system over time. The parties to the United Nations Framework Convention on Climate Change (UNFCCC) are also likely to include indicators in the "global stocktake," an assessment made every 5 years to measure progress under Article 14 of the Paris Agreement (United Nations 2015a). The ongoing negotiations on how to structure this process and on what information to include in the stocktake are due for finalization before the first stocktaking exercise takes place in 2023.

The main framework for determining key variables representing the state of the climate system has hitherto been the Global Climate Observing System (GCOS) set of essential climate variables (ECVs) (Bojinski et al. 2014; Table 1), a concept which dates from the early 2000s. This set consists of 54 different variables (16 atmospheric, 19 ocean, and 19 terrestrial), some of which have multiple indicators associated with them, and includes variables that are measured using conventional surface and upper-air meteorological observations, as well as many that are primarily measured using means such as remote sensing platforms or ocean-based platforms. An assessment of how well ECVs are monitored forms the core of regular assessments of the status of the global climate observing system (e.g., WMO 2015). Some variables, such as surface temperature, are supported by the comprehensive global observing networks, a long history of observations, and well-established mechanisms for international

Table 1. The current ECVs.

Category	Subcategory	ECVs
Atmospheric	Surface	Precipitation; pressure; temperature; surface radiation budget; wind speed and direction; water vapor
	Upper atmosphere	Earth radiation budget; lightning; temperature; water vapor; wind speed and direction
	Atmospheric composition	Aerosols properties; carbon dioxide, methane, and other greenhouse gases; cloud properties; ozone; precursors (supporting the aerosols and ozone ECVs)
Oceanic	Physics	Ocean surface heat flux; sea ice; sea level; sea state; sea surface salinity; sea surface temperature; subsurface currents; subsurface salinity; subsurface temperature; surface currents; surface stress
	Biogeochemistry	Inorganic carbon; nitrous oxide; nutrients; ocean color; oxygen; transient tracers
	Biology/ecosystems	Marine habitat properties; plankton
Terrestrial		Aboveground biomass; albedo; anthropogenic greenhouse gas fluxes; anthropogenic water use; fire; fraction of absorbed photosynthetically active radiation (FAPAR); glaciers; groundwater; ice sheets and ice shelves; lakes; land cover; land surface temperature; latent and sensible heat fluxes; leaf area index (LAI); permafrost; river discharge; snow; soil carbon; soil moisture

data exchange and archiving, while for some other variables (particularly ocean and terrestrial variables), the amount of information available is much more limited.

The ECVs provide the basis for a comprehensive assessment of the state of the global climate system, but form a complex picture, particularly for communicating with policymakers and nonspecialists. Frequently in public discourse, assessments like the WMO State of the Global Climate statement and similar reports are communicated via a single indicator, global mean surface temperature. To address this, WMO, in conjunction with the World Climate Research Programme (WCRP) and GCOS, developed a new set of headline climate indicators. The primary objective (Williams and Eggleston 2017) is to provide a range of indicators which gives a more comprehensive picture of the overall state of the global climate system than surface temperature alone. These indicators should be scientifically robust and cover the atmosphere, ocean, and cryosphere, while still being sufficiently simple and few in number (ideally between 5 and 10) to be suitable for widespread public communication. The indicators are targeted particularly at high-level policy events such as the activities of the UNFCCC, but we expect that they will also be valuable for broader reporting of the state of the global climate.

The desired characteristics (Williams and Eggleston 2017) for the headline climate indicators were as follows:

Relevance: Each headline indicator should be a clear, understandable indicator of the state of the climate system, with broad relevance for a range of audiences, whose value can be expressed as a single number. Some such global indicators may also have value at the national and regional levels.

Representativeness: The indicators as a package should provide a representative picture of a broad range of changes to the Earth system related to climate change.

Traceability: Each indicator should be calculated using an internationally agreed upon (and published) method and accessible and verifiable data.

Timeliness: Each indicator should be calculated regularly (at least annually), with the minimum possible time between the end of the period and publication of the data.

Data adequacy: The available data needed for the indicator calculation must be sufficiently robust, reliable, and valid.

Seven headline indicators (Table 2), each of which draws on one or more ECVs, were finalized by the WMO's Commission for Climatology at its 2018 meeting (WMO 2018a), following earlier discussions at meetings of WMO and GCOS in February (WMO 2017a; GCOS 2017) and October 2017. These took the above criteria into account while providing the broadest possible picture of the state of the climate system. These were first formally reported by WMO (for the five indicators which at that time had available data for 2017) in the 2017 State of the Climate report (WMO 2018c).

Table 2. The seven headline climate indicators.

Variable	Proposed indicator
Temperature	Global mean surface temperature
Ocean heat content	Global ocean heat content anomaly
Sea level	Global mean sea level change from a reference benchmark
Sea ice extent	Sea ice extent for the Arctic and Antarctic
Glacier mass balance	Global mass change of glaciers outside the Greenland and Antarctic ice sheets
Ocean acidification	Global mean ocean pH
Greenhouse gas mole fractions	Mean global mole fraction of CO_2

The purpose of this paper is to assess how well each of the seven indicators chosen by WMO is supported by the underlying observation and computational methodology, and, for some of the less completely observed indicators, what is required to improve their monitoring into the future to allow the criteria above to be fully met. The indicators are intended for use of global level; while many of them will also be applicable at smaller spatial scales, other indicators will also be required for local climate assessment. There are numerous other potential indicators, especially for atmospheric variables, which broadly meet the criteria above (see Table ES2 in the supplemental material) but have not been included in the interests of keeping the total number of indicators manageably small.

The way in which these indicators are conventionally expressed varies from indicator to indicator. For example, mean global mole fraction of CO_2 is most often expressed as absolute value, glacial mass balance as a year-on-year change, and temperature as an anomaly or departure from the average of a given baseline period. The choice of baseline period depends on the indicator and the availability of data. The most commonly used baseline period is 1981–2010 (WMO 2017b), especially for indicators which draw on satellite datasets which begin in the 1970s, while another example of a baseline period, used particularly for temperature, is 1850–1900, used as an approximation to preindustrial conditions by IPCC (Allen et al. 2018). The choice of baseline shifts absolute values but has little or no impact on the estimation of changes or trends.

The headline indicators

Temperature. Global mean surface temperature (GMST) is arguably the best-known metric used in monitoring the state of the climate. Conventionally, it is defined using a combination of air temperature at screen level (2 m) over land and sea surface temperature (SST) in ocean areas. It is conventionally expressed as an anomaly from a baseline period, although the baseline period used differs between different datasets.

A number of global datasets are maintained by various institutions (see Table ES1 in the supplemental material). These combine historical data drawn from a range of sources with data collected through national meteorological services and transmitted in near–real time through the WMO's Global Telecommunications System, particularly the monthly CLIMAT reports from land stations, while the International Comprehensive Ocean–Atmosphere Dataset (ICOADS; Freeman et al. 2017) is a major data source for SST data. More recently, reanalyses have also been used for the assessment of global temperatures, using the (not strictly equivalent) definition of air temperature over the oceans rather than SST. As updating is drawn from sources which normally report within a few days of the end of each month, these GMST analyses are normally available for each month within 1–2 weeks of the end of the month for reanalyses, and 2–4 weeks for "conventional" datasets.

All of the datasets listed in Table ES1 have been the subject of extensive assessment of their quality and homogeneity. The largest differences between them, particularly in more recent years, relate to the way in which they do (or do not) interpolate over data-sparse areas such as the polar regions, with approaches ranging from that of HadCRUT4 (which treats 5° × 5° grid boxes with no data as missing) to the reanalyses, whose data are spatially complete (Fig. 1), and Cowtan and Way (2014), who use satellite data to extend surface analyses to polar regions. As the Arctic is warming much faster than the rest of the globe (Davy et al. 2018), the more spatially complete datasets show stronger recent warming trends than those with limited Arctic representation (Simmons et al. 2017). The treatment of systematic biases associated with changes in the way that SST are measured is also significant (e.g., Kennedy et al. 2019).

Current values of GMST can be linked to the preindustrial period with a modest level of uncertainty (Hawkins et al. 2017). Although the preindustrial period was not formally

defined in the Paris Agreement, IPCC has adopted 1850–1900 as a working definition of a preindustrial-equivalent baseline. Of the datasets in Table ES1, only HadCRUT4 and BEST cover the full 1850–1900 period, with other conventional datasets starting in 1880, but methods have been developed (Allen et al. 2018) to connect those datasets (and the reanalyses) to a 1850–1900 baseline. Uncertainties in instrumental GMST in the 1850–1900 period, particularly the early part of it, are larger than for more recent data, because of sparse data coverage (especially for Southern Hemisphere land areas), and potential residual uncertainties associated with nonstandardization of instrument shelters and SST measurement methods (Morice et al. 2012).

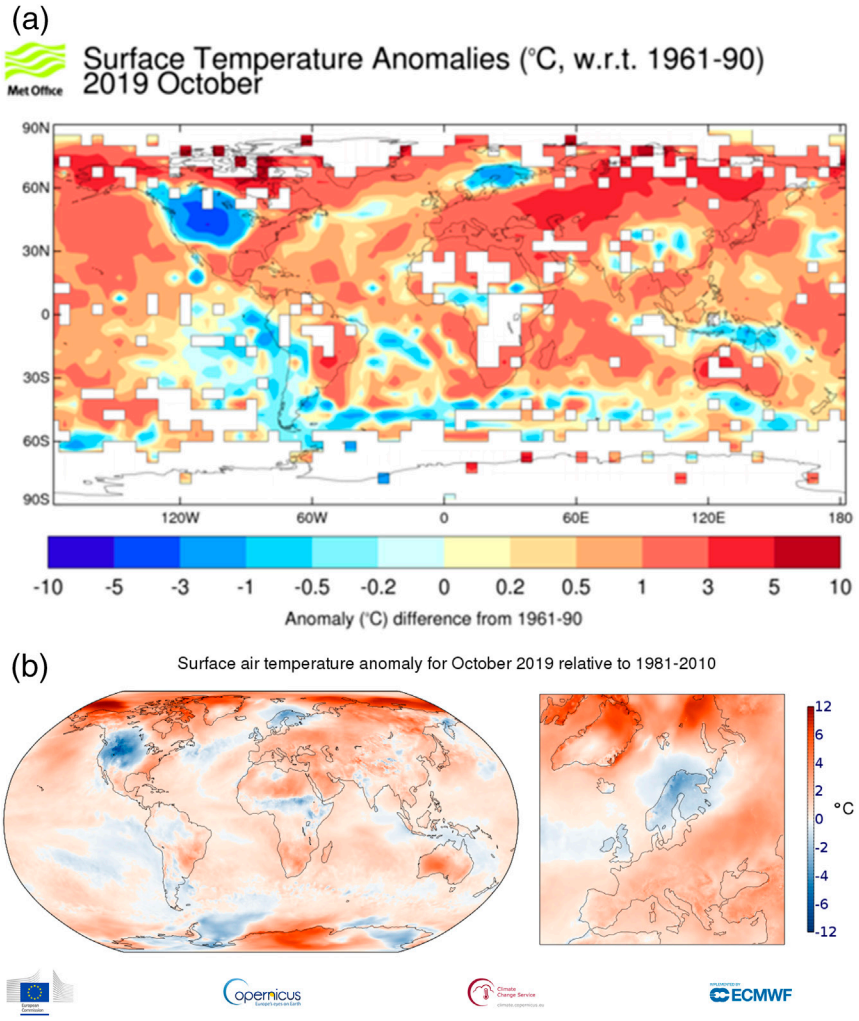

Fig. 1. October 2019 global temperature anomaly (°C) maps showing differing coverage in different datasets: (a) the HadCRUT4 dataset (Met Office) and (b) the ERA5 dataset (Copernicus Climate Change Service/ECMWF). The ERA5 dataset shows more extensive coverage in polar regions and over Africa than does HadCRUT4. This also illustrates the different baseline periods used by different data providers in their routine products.

Ocean heat content. A defining characteristic of the global ocean is a large capacity to store and transport heat. The upper few meters of the global ocean have the same heat capacity as the entire atmosphere (Gill 1982). It is estimated that over 90% of the radiative imbalance associated with anthropogenic climate change is absorbed by the oceans, with the remaining 10% going into heating of the land surface, atmosphere, and cryosphere (von Schuckmann et al. 2016). The ocean's dominant role in the planetary energy budget arises at annual time scales (Palmer and McNeall 2014) and makes ocean heat content (OHC) change a primary observational metric of global warming because it provides a strong constraint on the magnitude of Earth's energy imbalance (von Schuckmann et al. 2016; Palmer 2017). In addition, OHC is less subject to interannual to decadal variability than global mean surface temperature (Palmer and McNeall 2014; Wijffels et al. 2016).

The primary means of estimating OHC change is through analysis of historical subsurface temperature profiles. The methods used are broadly similar to those applied to global surface temperature; a number of profiles in a given time "window" are spatially interpolated to estimate the global average, relative to a reference period. As with surface temperature, interplatform biases are assessed and corrected for, e.g., those associated with expendable bathythermograph (XBT) instruments (Abraham et al. 2013; Cheng et al. 2016). A number of indirect methods for estimating OHC change are also available, such as satellite-based

estimates of ocean thermal expansion and ocean data assimilation products that combine the available observations with a dynamical ocean model (Meyssignac et al. 2019).

A key challenge for estimating OHC change is the highly heterogeneous and depth-limited historical ocean sampling (Abraham et al. 2013; Palmer 2017). Estimates of annual OHC change that extend back to the mid-twentieth century (Fig. 2) are typically limited to the 0–700-m-depth layer and have particularly large sampling uncertainties before the mid-1960s (Lyman and Johnson 2008; Palmer and Brohan 2011; Abraham et al. 2013; Cheng et al. 2017). Since the mid-2000s, the Argo array of autonomous profiling floats has provided near-global coverage of the upper 2,000 m of the ice-free ocean and a dramatic improvement in our ability to monitor OHC change (Riser et al. 2016), with greater consistency between data products.

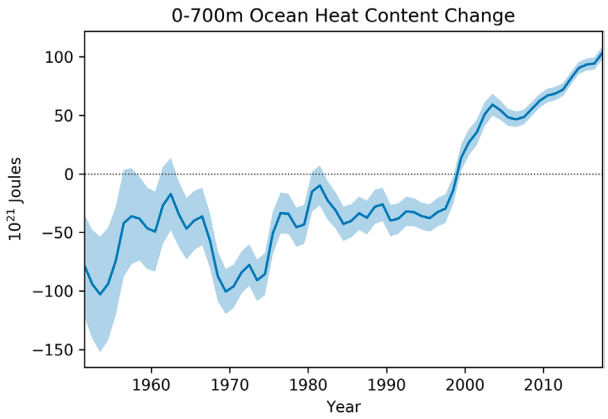

Fig. 2. Time series of 0–700-m-depth global ocean heat content change (10^{21} J) relative to the 1981–2010 average, based on the EN4 quality-controlled subsurface ocean temperature profiles (Good et al. 2013) following Palmer et al. (2007). The shaded regions indicate the 5th–95th percentiles of uncertainty, following the approach of Palmer and Brohan (2011). Note that uncertainties associated with bias correction and structural uncertainty are not represented. A 1–2–1 smoothing has been applied to the annual data to reduce sampling noise. Source: Good et al. (2013).

Estimates of sub-2,000-m OHC change rely on a sparse network of full-depth hydrographic sections from scientific research vessels that permit estimation of decadal trends in OHC from about the 1990s onward (Purkey and Johnson 2010; Desbruyères et al. 2016). However, combined with Argo observations, this information allows us to estimate the global OHC change over the full-depth from the mid-2000s and also characterize the spatial time evolution of the warming (Desbruyères et al. 2017). While the observational basis is less robust, some recent estimates of full-depth OHC change extend back to 1960 (Cheng et al. 2017).

Time series of global OHC anomaly from a number of semi-operational products are presented routinely as part of the annual BAMS State of the Climate report (e.g., Blunden et al. 2018). The data include annual time series for the 0–700 and 700–2,000-m layers, and an estimate of the long-term trend for ocean below 2,000 m. The data products are based on various interpolation methods and may also vary in their approach to XBT bias correction (Boyer et al. 2016). While statistically based estimates remain prevalent for monitoring OHC change, ocean data assimilation products (ocean reanalyses) are also increasingly being used (e.g., Palmer et al. 2017). An ensemble of four ocean reanalyses is used to provide annual time series of global OHC change for the 0–700 and 0–2,000-m layers from 1993 onward as part of the Copernicus Marine Service Ocean State Report (von Schuckmann et al. 2018).

Linking the current OHC state robustly to the preindustrial climate is extremely challenging, owing to the lack of subsurface temperature observations during the period 1850–1900. The primary source of data we have in this regard is the HMS *Challenger* expedition, which took place between 1872 and 1876. Although the *Challenger* subsurface temperature observations were global in scope, they were taken along a small number of ship tracks, mostly confined to 40°N–40°S in the Atlantic and Pacific Oceans (Roemmich et al. 2012). These data have been used to assess the change in OHC for 0–700 m between 1872–76 and 2004–10 (Roemmich et al. 2012), albeit with large uncertainties. Further insights into the OHC state during preindustrial times may be afforded by more novel approaches, such as the Green's function method used by Zanna et al. (2019). This method uses an estimate of ocean circulation to propagate observed surface temperature anomalies into the ocean interior and therefore

provide an estimate of change in ocean heat content since 1871.

Since the mid-2000s, Argo provides the vast majority of subsurface temperature profiles used for in situ–based estimates of OHC change. While these data are provided in near–real time, the highest quality "delayed-mode" data (Wong et al. 2018) may have a 1–2-yr time lag associated with them. Public release of research cruise data are often the responsibility of the cruise principal investigator and can result in delays of several years.

Sea level. The global mean sea level (GMSL) is recognized as a leading indicator of global climate change because it reflects changes occurring in multiple different components of the climate system (ocean, atmosphere, cryosphere, and hydrosphere) and their mutual interactions.

Historically, sea level has been measured by tide gauges located along continental coastlines and islands but the coverage of long, good-quality tide gauges is heterogeneous and biased toward the Northern Hemisphere for most of the twentieth century. This tide gauge–based sea level record, despite its limited geographical coverage, provides a fundamental historical reference for long-term sea level studies. Since the early 1990s, sea level is routinely monitored with near-full global coverage by high-precision satellite altimetry (Fig. 3) that provides

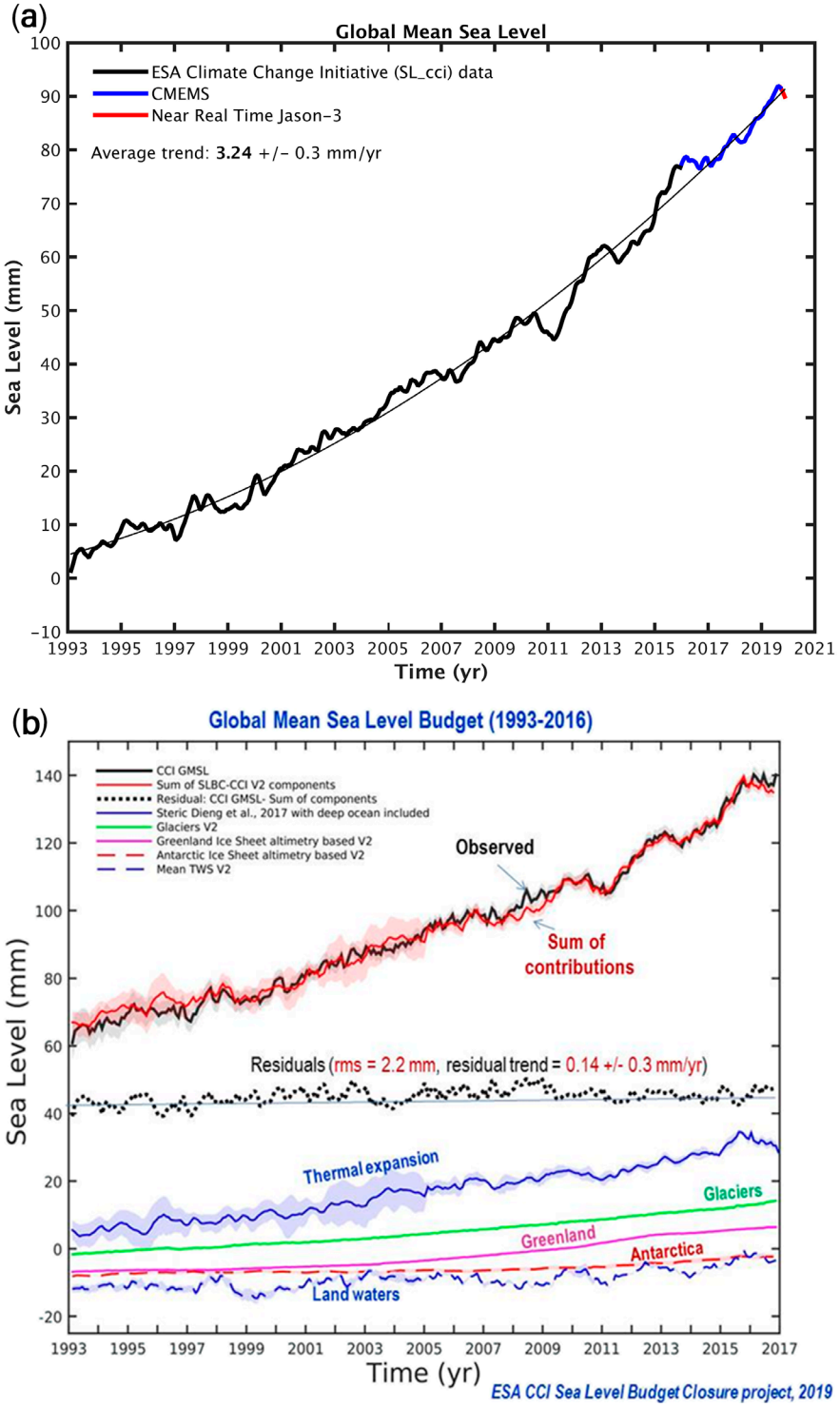

Fig. 3. (a) Global mean sea level evolution over January 1993–December 2019 based on multi-mission satellite altimetry. From January 1993 to December 2015, the curve is derived from the ESA Climate Change Initiative sea level product (Legeais et al. 2018). Beyond December 2015, it is extended with sea level data from the Copernicus Marine Environment Monitoring Service (www.marine.copernicus.eu). The last few points of the time series (in red) are based on the near-real-time altimetry measurements of the *Jason-3* satellite (Source: Laboratoire d'Etudes en Geophysique et Oceanographie Spatiales, EGOS). (b) Global mean sea level budget over 1993–2016. The individual contributions are shown at the bottom of the panel. The altimetry-based sea level and sum of contributions are shown by the black and red curves, respectively (Source: ESA Sea Level Budget Closure project, Horwath et al. 2020).

"absolute" sea level data in a geocentric reference frame (unlike tide gauges that also sense vertical land motions). This allows the routine estimation of GMSL as a climate indicator from 1993 onward.

Since the launch of the TOPEX/Poseidon mission in 1992, there is now a 27-yr-long sea level record from which the global mean sea level rise can be inferred as well as regional trends (Cazenave et al. 2019). The satellite altimetry constellation includes the so-called "reference" missions (TOPEX and *Jason-1*, *-2*, and *-3*, covering the 66°N–66°S latitude domain, and providing the most accurate long-term stability of sea level measurements at global and regional scales). There are also complementary satellites covering part of the Arctic Ocean, up to 82°N latitude (*ERS-1* and *-2*, *Envisat*, *SARAL*/AltiKa, *Sentinel-3A* and *-3B*). Different groups worldwide provide altimetry-based GMSL time series, which can be updated with less than 1 month's delay using *Jason-3* data, as well as gridded datasets. Although different processing approaches are implemented by these groups, the quality of the different GMSL time series is similar. Long-term trends agree well to within 6% of the signal, approximately 0.2 mm yr^{-1} in terms of trend, well within the GMSL trend uncertainty range estimated to around 0.3 mm yr^{-1} from tide gauge comparison and error assessments of all sources of uncertainties affecting the altimetry system.

This 27-yr-long record indicates that the global mean sea level continues to rise at a mean rate of 3.2 ± 0.3 mm yr^{-1}, with some evidence of acceleration. The acceleration (about 0.1 mm yr^{-2}) results of increased ocean thermal expansion (due to ocean warming) and ice mass loss from glaciers, Greenland, and Antarctica (WCRP Global Sea Level Budget Group 2018; Nerem et al. 2018).

Regular assessments of the global mean sea level budget have been recently initiated for the altimetry era, a period for which different observing systems are available (e.g., Argo profiling floats for the ocean thermal expansion component and GRACE space gravimetry for the mass components). These budget studies that indicate that in terms of global mean, the sea level budget is closed within quoted uncertainties (e.g., WCRP Global Sea Level Budget Group 2018; Horwath et al. 2020) are important for many reasons. Quasi closure of the sea level budget indicates that no systematic errors affect the different observing system and that there is no important missing contribution (e.g., from the deep ocean not sampled yet by Argo). They allow improved process understanding and detection of temporal change (e.g., acceleration or abrupt change) in the components, and may be useful for validating the climate simulations used for projections (although the current record is still short for the latter application). Finally, the altimetry-based global mean sea level corrected for the mass components (e.g., the GRACE-based ocean mass contribution) is a proxy of the total ocean heat content. It provides thus another approach to monitor the global mean OHC, independently from in situ ocean temperature measurements, with applications for estimating the Earth's energy imbalance (von Schuckmann et al. 2016).

While the GMSL remains a major climate indicator, for coastal communities, what matters is "relative" coastal sea level change ("relative" means with respect to the Earth crust), i.e., the sum of the GMSL plus superimposed regional variability plus small-scale coastal processes. The latter include small-scale shelf currents, changes in wind and waves, and freshwater input from river estuaries (that modifies the density structure of seawater). Moreover, at the coast, vertical land motions due to natural or anthropogenic factors (such as ground subsidence from hydrocarbon or water extraction, or sediment compaction in river deltas) will superimpose on the global mean and regional sea level components. Such vertical land motions amplify the climate-related sea level rise in many places, although in others they offset it.

Sea ice extent. Sea ice extent is the most widely used climate indicator to assess long-term changes in Arctic and Antarctic sea ice. Sea ice extent is defined as the area covered by an areal

ice concentration greater than 15%. It is typically derived from passive microwave satellite measurements that are available in close to real time and provide a consistent observational record that now spans more than 40 years. There are several different sea ice datasets that make use of passive microwave satellite measurements, and different retrieval algorithms. Therefore, the uncertainty varies depending on the dataset. Resolving the position of ice edge or marginal ice zone, thin ice and melt ponds forming on the surface of the sea ice are the primary sources of uncertainty (Ivanova et al. 2015; Comiso et al. 2017). To that end, the differences in sea ice extent between datasets can range from 0.5×10^6 to 1×10^6 km^2 (Meier and Stewart 2019). Further, construction of more than 40 years of sea ice extent record requires combining sensors of shorter operational lifetimes together; therefore, uncertainty can vary temporally depending on the quality of sensor calibration (Eisenman et al. 2014). Despite these differences, the long-term datasets of passive microwave satellite derived measurements of sea ice extent still provide the most robust and consistent indictor of long-term change (Comiso et al. 2017).

Figure 4 shows the time series of sea ice extent anomalies for the Arctic in March (winter maximum) and September (summer minimum) as well as for the Antarctic in September (winter maximum) and February (summer minimum) for two of the most common, widely used, and available in close to real time sea ice extent datasets, the Sea Ice Index version 3 (Fetterer et al. 2017) and Satellite Application Facility on Ocean and Sea Ice (OSI-SAF) version 2 (Lavergne et al. 2019). Note the interannual variability is similar between these two products. In the Arctic, the summer minimum sea ice extent has declined at a rate of around 12.5% decade^{-1} and winter maximum sea ice extent has declined at a rate of around 2.7% decade^{-1} over the 1979–2019 period. Reductions are particularly prominent in the Beaufort and Chukchi Seas during the summer and in the Barents and Bering Seas during the winter. Overall, the downward trend in the Arctic's September sea ice extent is perhaps one of the most visually striking indicators of climate change. In the Antarctic, there has been considerably more interannual variability in both summer and winter sea ice extents in addition to a weak increasing trend up until 2014 that contrasts the strong negative trend in the Arctic. However, this positive Antarctic trend has been found to have reversed in 2014 with the recent decreasing sea ice extent rates greater than observed in the Arctic (Parkinson 2019).

There is evidence to suggest that the recent decline in Arctic September sea ice extent observed over the post-1979 satellite record is unprecedented compared to historical reconstructions for the pre-1979 period (Walsh et al. 2017) and paleoclimate proxy data (e.g., Kinnard et al. 2011). Pre-1979 observations for the Antarctic point to a decrease in February sea ice extent (Abram et al. 2013; Gallaher et al. 2014), but there is considerable uncertainty in these observations and therefore it is difficult to link these with the more consistent post-1979 satellite observations (Hobbs et al. 2016).

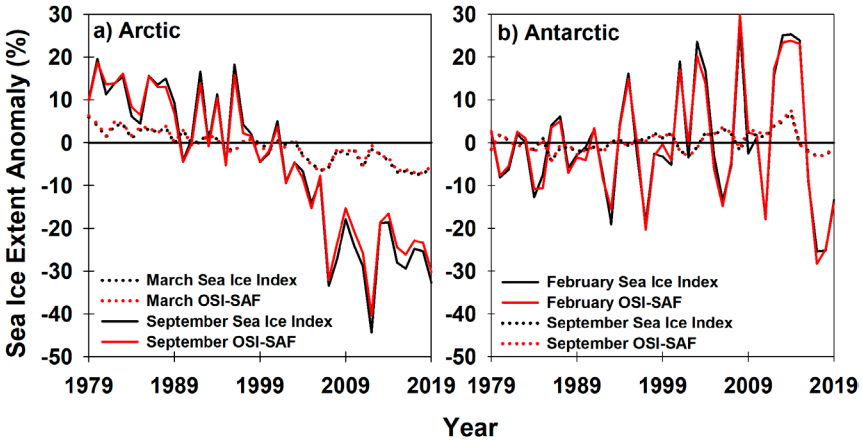

Fig. 4. Time series of 1979–2019 sea ice extent anomalies (%) in (a) March (maximum ice extent) and September (minimum ice extent) for the Arctic and (b) September (maximum ice extent) and February (minimum ice extent) for the Antarctic. The anomaly for each year is the percentage difference in sea ice extent relative to the 1981–2010 mean. Sea ice extent is defined as an area covered by sea ice that contains an ice concentration of 15% or greater. Data source: Sea Ice Index version 3 (Fetterer et al. 2017) and OSI-SAF version 2 (Lavergne et al. 2019).

A concern with the 40+-yr passive microwave sea ice extent record is that the remaining satellites in orbit are well beyond their operational lifetime (Witze 2017). However, the European Organization for the Exploitation of Meteorological Satellites (EUMETSAT) Polar System–Second Generation (EPS-SG), which is expected to launch in 2023, will contain sensors to facilitate the continuation of the 40+-yr passive microwave sea ice extent record. In addition, there is the Copernicus Imaging Microwave Radiometer (CIMR) mission that is currently a candidate mission (high priority) within the European Copernicus Expansion program and could launch in the late 2020s. Should the current passive microwave sensors in orbit fail before these aforementioned European satellites are launched, gap-filling data are currently available from the *Fengyun 3* (*FY-3*) Microwave Radiation Imager (MWRI) operated by the China Meteorological Administration (CMA).

Glacier mass balance. Variations in glacier mass are closely linked to changes in atmospheric forcing. The mass balance of glaciers—defined as the sum of all gains and losses in ice mass—is primarily affected by summer air temperatures. Variations in solid precipitation and radiation fluxes also exert a significant influence on glacier mass change (Braithwaite 1981; Ohmura 2001). Long-term cumulative glacier mass changes are thus a valuable indicator integrating the effects of various components of the global climate system on snow and ice. As glaciers adapt to altered climatic conditions by retreating to higher elevation, the mass change signal also depends on their dynamic response. Glaciers are distributed over most continents of the Earth with a concentration in the high mountain ranges of Asia and North and South America, as well as in high latitudes (Pfeffer et al. 2014). Limited glacierization is, however, also present in tropical regions.

Observing the mass change of the roughly 200,000 glaciers outside the two ice sheets in Greenland and Antarctica is challenging due to their remoteness and general inaccessibility on the one hand, meaning that sampling of these glaciers is incomplete, and on the other hand due to the inherent difficulty of directly measuring variations in glacier mass. Therefore, a combination of different methodologies is employed. Direct field observations on about 300 glaciers globally deliver data on seasonal to annual glacier mass change (Zemp et al. 2015). Due to logistical reasons, most observations refer to glaciers smaller than about 20 km^2, although in several regions larger glaciers are also monitored. Although at least one series is available in all large-scale glacierized regions worldwide, measurements are overrepresented in the European Alps, Scandinavia, and the Rocky Mountains. Due to the inhomogeneity of national monitoring programs and the laborious field data processing, global-scale results on seasonal or annual mass change are typically only available a few months up to a year after acquisition. Comparison of repeated digital elevation models of the ice surface, referred to as the geodetic method, allows assessing the volume change of large glacier samples at time intervals of a few years to decades (e.g., Kääb et al. 2012; Brun et al. 2017; Braun et al. 2019). The Gravity Recovery and Climate Experiment (GRACE) provided a powerful method to directly observe glacier mass change from space, albeit only at a spatial resolution of 100 km or more, until its cessation in 2017. Furthermore, uncertainties for mountain ranges with small glaciers are high due to limitations in the model separating mass change signals from glaciers and other components of the hydrological cycle (e.g., Gardner et al. 2013; Wouters et al. 2019).

Data on glacier mass balance (Fig. 5) are collected through a worldwide network of national correspondents and principal investigators and are further distributed by the World Glacier Monitoring Service (WGMS, www.wgms.ch). Analysis of long-term variations in glacier mass often relies on a set of global reference glaciers, being defined as sites with continuous high-quality in situ observations of more than 30 years. Results from these series are, however, only partly representative for glacier mass changes at the global scale as they are

disproportionately in well-accessible regions (e.g., Europe). For the most recent pentad 2015–19, data of WGMS reference glaciers indicate specific mass-change rates that are more negative than in all other periods since 1950 (Fig. 5a). These measurements corroborate the widespread and substantial glacier mass losses recognized for several decades.

Global mass change estimates require extrapolation of the scattered direct observations to all glaciers. The study by Zemp et al. (2019) provides a comprehensive assessment of glacier mass changes at the global scale based on a combination of year-to-year variabilities stemming from in situ measurements, and decadal-scale geodetic mass changes from a large set of roughly 20,000 individual glaciers covering about 25% of the global glacier area. Results indicate an acceleration of glacier mass losses from around 1985, after moderately negative values (Fig. 5b). Over the last decade, glaciers lost more than 300 Gt yr^{-1} on average, thus approaching a sea level rise contribution of 1 mm yr^{-1} (Zemp et al. 2019). Mass loss from glaciers outside the two ice sheets thus makes up almost a third of the current sea level rise. The glacier mass-change rates for the last decade are also confirmed by global studies based on satellite gravity and altimetry (Fig. 5b; Gardner et al. 2013; Wouters et al. 2019).

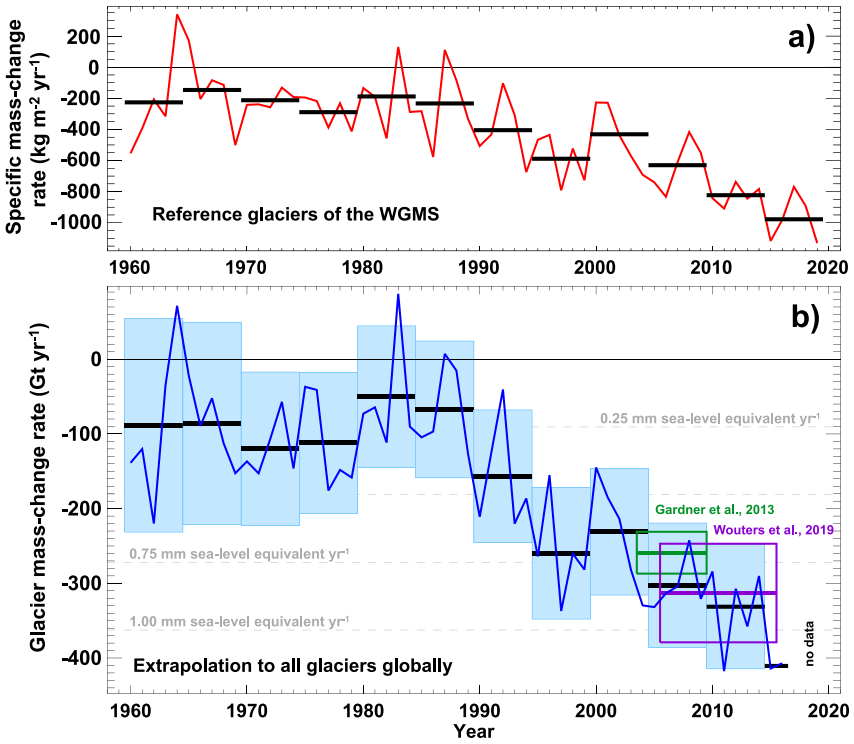

Fig. 5. (a) Average of observed annual specific mass-change rate (red; kg m^{-2} yr^{-1}) of all reference glaciers of the WGMS, including pentadal means (black lines). (b) Annual mass-change rate (Gt yr^{-1}) of all glaciers outside the two ice sheets (Greenland, Antarctica) inferred from a combination of remotely sensed glacier thickness change and annual in situ observations, according to Zemp et al. (2019). Pentadal averages (black lines) and their uncertainties (shading) are shown. Global glacier mass-change rates from two independent studies, primarily based on GRACE results, are shown for comparison [2003–09 for Gardner et al. (2013); 2006–16 for Wouters et al. (2019)]. Note that results of Wouters et al. (2019) do not include glaciers in the periphery of Greenland and Antarctica, which have been supplemented for comparability based on Zemp et al. (2019). Source: World Glacier Monitoring Service.

Knowledge on glacier mass change is limited before the 1960s. Only very few direct observations exist, and the spatial coverage of these measurements does not allow any global assessment. However, observations of glacier length change reaching back until the sixteenth century in some cases (Leclercq et al. 2014), as well as glacier modeling (e.g., Marzeion et al. 2014) indicates significant glacier mass losses globally since the maximum of the so-called Little Ice Age around 1850. This is also consistent with geomorphological evidence (Grove 2004).

Ocean acidification. Increasing atmospheric carbon dioxide concentrations affect the chemistry of the ocean. The ocean absorbs around 30% of the annual emissions of carbon dioxide (CO_2) to the atmosphere, which helps to alleviate the impacts of climate change on the planet. The CO_2 reacts with seawater and alters the acidity of the ocean by decreasing its pH. This process is called ocean acidification. The change of pH level is linked to a range of shifts in other carbonate chemistry parameters in the seawater, such as a decrease in carbonate

ion concentrations. This lowers the saturation state of biogenic calcium carbonate minerals, including calcite and aragonite, used in the formations of shells and skeletal material by a variety of marine organisms, from mussels and crustaceans to corals, decreasing their ability to calcify (e.g., reef building corals and shelled mollusks). Together, the changes in CO_2 concentration, pH, and carbonate chemistry parameters affect the energy budget of marine life, lessening the potential to grow and reproduce. It is therefore important to fully characterize the ocean's changing carbonate system through observations with high temporal and spatial resolution.

Ocean acidification observations started at a limited number of stations 30 years ago, a very limited set of observations compared with the other headline indicators, and at present data are generally reported at the station level rather than as a consolidated global indicator. Established methodology and standards are available, but data are not regularly produced by countries. IPCC (2019a) reported information on ocean pH based on eight stations globally with 15 years or more of data.

Notwithstanding the limited existing data, increasing awareness, international collaboration, e.g., that supported by the Intergovernmental Oceanographic Commission–United Nations Educational, Scientific and Cultural Organization (IOC-UNESCO), the Ocean Acidification International Coordination Centre (OA-ICC) and in particular the Global Ocean Acidification Observing Network (GOA-ON), and related capacity development activities, have increased the human and technical capacity to measure ocean acidification and analyze related datasets. In 2015, ocean acidification was further identified as one topic to address within the 2030 Agenda for Sustainable Development (United Nations 2015b) [Sustainable Development Goal (SDG) target 14.3]. In 2017 UN Member States further agreed on the related indicator 14.3.1: *average marine acidity (pH) measured at agreed suite of representative sampling stations*. IOC-UNESCO is the custodian agency for this SDG indicator, which means it is responsible to develop internationally agreed-upon standards, coordinate the indicator development, and support increased adoption and compliance with the internationally agreed standards at the national level. Based on this methodology, IOC-UNESCO collects ocean acidification data from countries (or regional organizations) through existing mandates and reporting mechanism to provide internationally comparable data and calculate global and regional aggregates. The commissions also strengthen national statistical capacity and improve reporting mechanisms for ocean acidification with specific capacity training activities. As a result of these initiatives, it is expected that the observation network for ocean acidification will expand rapidly over the next few years.

In 2019, a new 14.3.1 data portal[1] was launched by IOC-UNESCO, which now facilitates the reporting and analysis of ocean acidification data and metadata toward reporting of the indicator. In turn, a headline indicator on ocean acidification can benefit from the collected data on an annual basis by IOC-UNESCO, assuring a high quality of scientific data and information used across different reporting mechanisms, international conventions, and related publications/outputs.

[1] www.goa-on.org

Greenhouse gas concentration. Carbon dioxide is the single most important anthropogenic greenhouse gas in the atmosphere, contributing ~66% of the radiative forcing by long-lived greenhouse gases. It is responsible for about 82% of the increase in radiative forcing over the past decade and about 81% of the increase over the past 5 years. Atmospheric concentration of CO_2 is closely linked to anthropogenic activities and it is defined by the exchange processes between the atmosphere, the biosphere, and the oceans.

The long-term trends and seasonal variations in the global average mole fractions of CO_2 (Fig. 6) are calculated using surface observations at stations of the Global Atmosphere Watch (GAW) Programme and its contributing networks. In total 129 stations were used for the

calculation of the 2018 global average. For the global analysis (WMO 2009) used in the WMO Greenhouse Gas Bulletin, stations were selected to be representative of their region and not significantly impacted by local CO_2 sources or sinks (e.g., not impacted by direct emissions from the traffic or industry or direct CO_2 uptake by the forest).

Data from the network are submitted to the WMO World Data Centre for Greenhouse Gases within 8 months after the end of the calendar year, after receiving a thorough quality control by the laboratories performing the measurements. Some stations provide data on their websites in shorter release cycles with delays up to just 1 day, bypassing part of the quality protocols, but only the fully quality controlled data can be used for the global mean calculations.

All WMO GAW greenhouse gas observations are performed following the recommendation for quality assurance, in particular the confirmed traceability chain to the primary WMO scale, as described in WMO (2018b). To ensure global compatibility of the measurements, the World Calibration Centre (WCC), supported by NOAA, organizes regular comparisons in which the set of the well-characterized cylinders is sent by the world calibration center to the stations in the chain (so that stations measure the same flasks one after the other). This demonstrates the compatibility of the measurement systems.[2]

Selection of observational sites is based on whether they provide data representing a reasonably large geographical area, considering the fact that some sites may be susceptible to local emission sources and sinks.

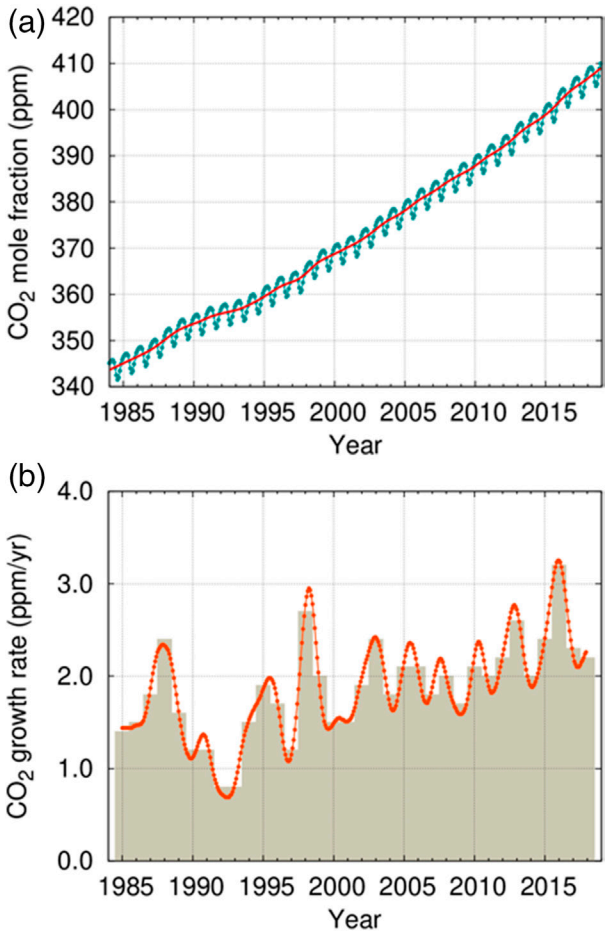

Fig. 6. (a) Monthly globally averaged CO_2 mole fraction (ppm) and (b) its growth rate (ppm yr^{-1}) from 1984 to 2018. Increases in successive annual means are shown as the shaded columns in (b). The red line in (a) is the monthly mean with the seasonal variation removed; the blue dots and line depict the raw monthly averages. Source: World Meteorological Organization Greenhouse Gas Bulletin (https://public.wmo.int/en/resources/library/wmo-greenhouse-gas-bulletin).

The mole fractions of greenhouse gases exhibit variations on different time scales. The two major components are seasonal variation and long-term trends. In the WMO Greenhouse Gas Bulletin, average seasonal variations derived from components of Fourier harmonics and long-term trends are extracted via a Lanczos low-pass filter.

In general, the number and distribution of sites used to assess trends during the analysis period should be kept unchanged as much as possible to avoid biases and additional uncertainties arising from introduction of the new data of removal of stations. However, data covering the entire analysis period are available for fewer than 20 sites[3]; for most sites, coverage is for shorter periods or contains data gaps. Smaller gaps are filled using linear interpolation based on available data in the fitted long-term trends derived by subtracting the average seasonal variation.

Six zonal mean mole fractions are calculated by determining the arithmetic average of the mole fractions in each latitudinal zone (90°–60°, 60°–30°, and 30°–0° in each hemisphere), based on consistent datasets derived as above. Global and hemispheric means are calculated as the weighted averages of the zonal means taking account of the area of each latitudinal zone. Growth rates for the whole globe, each hemisphere and

[2] Results can be found on the WCC website at www.esrl.noaa.gov/gmd/ccgg/wmorr/wmorr_results.php

[3] https://gaw.kishou.go.jp/publications/summary

each latitudinal zone are derived from the time derivatives of the corresponding long-term trends fitted to the observations (WMO 2009). The uncertainty in global mean mole fractions (at a 68% confidence level) is calculated using bootstrap analysis. From the dataset of mole fractions obtained after the site selection and data extension procedure described above, *n* sites are randomly selected, with duplication of the same sites allowed on condition that at least one site is selected from each of the six latitudinal bands, and a global mean mole fraction is calculated using the data from the *n* sites. The procedure is repeated *m* times to determine *m* different global mean mole fractions. Uncertainty is defined as the standard deviation of these mole fractions.

The preindustrial levels of CO_2 are estimated with the same techniques as are used for modern in situ measurements but using analysis of the air trapped in ice cores. Those levels are estimated with a level of confidence which is lower than for modern observations (uncertainty of the global mean estimate is 0.1 ppm), but still high (Marcott et al. 2014). The 1750 globally averaged abundance of atmospheric CO_2 based on measurements of air extracted from ice cores and from firn is 278 ± 2 ppm (Etheridge et al. 1996).

Examples of variables not included in the key indicators

An important characteristic of the indicators selected is that they represent variables which can be expressed as a single number which is scientifically meaningful as an indicator of the state of the climate system. Some important variables in the climate system were not selected for the key indicators because they are not amenable to such a "single number" expression, or because they lack the global coverage necessary to be considered fully representative.

To illustrate these challenges, the question of whether the world is experiencing an intensification of the hydrological cycle is an important one in assessing climate change. At first glance, the most obvious indicator to report this would appear to be globally averaged precipitation, which was one of the indicators originally under consideration (WMO 2017a). However, whereas for most key climate indicators, most parts of the world are changing in the same direction, for precipitation, there are strong regional variations in the sign of observed changes (IPCC 2013), making regional signals of greater importance for many applications than an overall global signal.

Globally averaged precipitation on land is reported annually from a number of different datasets (Vose et al. 2018), while precipitation over the ocean, using satellite data alongside in situ observations is also reported from the satellite-based Global Precipitation Climatology Project (GPCP) dataset (Huffman et al. 2009). However, the spread between the land-based datasets is large in both historical (Herold et al. 2016; Gehne et al. 2016) and recent data—for example, the 2017 mean annual global precipitation over land reported in Vose et al. (2018) ranged from only slightly above average to the highest on record—while data over the ocean are only available during the satellite era. Reanalysis precipitation datasets also show a large degree of divergence (Alexander et al. 2020). Interannual variations in the distribution of precipitation over land and ocean are also strongly influenced by seasonal climate drivers (Gu and Adler 2011), such as El Niño–Southern Oscillation (ENSO), as well as longer-term forcings, complicating interpretation of global or semi-global means.

The seven headline indicators all reflect mean-state variables measured at seasonal and/or annual time scales. Many of the most significant impacts of climate change occur as a result of extreme events. It would be desirable, in that context, to include an indicator of the occurrence of extreme events as a key headline indicator. However, at present, the spatial coverage of routine reporting of extremes indices, such as the indices of temperature and precipitation extremes defined by the Expert Team on Climate Change Detection and Indices (ETCCDI), is limited, with recent analyses largely confined to Europe, North America, Australia, and parts of Asia (Perkins-Kirkpatrick et al. 2018; Tye et al. 2018; Fig. 7). This is largely due to

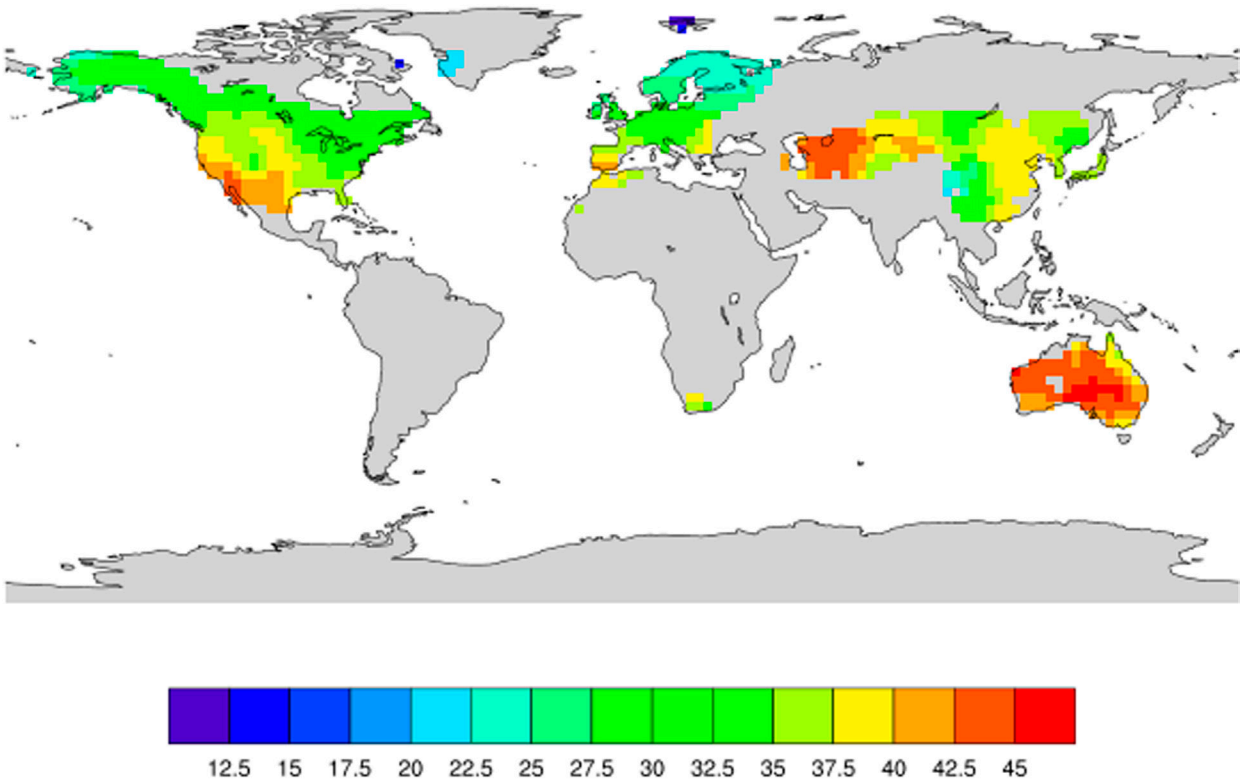

Fig. 7. The highest daily maximum temperature (°C) of 2017 from the gridded GHCNDEX extremes indices dataset (Donat et al. 2013), illustrating the limited coverage for extremes data in near–real time. (Source: University of New South Wales, through www.climdex.org).

the lack of a mechanism for routine reporting of the daily temperature and precipitation data needed for the calculation of these indices, combined with limited exchange of historical daily data, and limited updating of the indices datasets developed for many parts of the world in the 2000s through the ETCCDI series of workshops (Peterson and Manton 2008). WMO has recently introduced provisions for quality-controlled daily data to be exchanged routinely through the monthly CLIMAT messages and it is hoped that strong uptake of this will improve the capacity to monitor extremes in a timely manner, opening the possibility of regular reporting of one or more globally measured indicators of climate extremes in the future. Some use is also beginning to be made of reanalyses for reporting of indices of climate extremes (King et al. 2019).

Future opportunities and challenges

Observations are important for understanding the current trajectory of climate change. Global mean surface temperature is a key indicator used in the Paris Agreement, while the seven key indicators, along with other ECVs, are widely used in assessing whether observed climate change is consistent with model projections.

Our capacity to observe most of the variables used for assessment of the key climate indicators is improving over time. The introduction of Argo and related systems have greatly enhanced the monitoring of ocean-based indicators (e.g., Johnson et al. 2019), while remote sensing platforms have also made possible forms of monitoring which would not have been practical with traditional in situ measurements. Reanalyses also play an increasingly important role in operational climate monitoring products such as the WMO State of the Global Climate report and contribute to regular reporting of GMST. In situ measurements are still very important to the global observing system and are critical for assessment of global temperatures and greenhouse gas concentrations.

Maintenance of observing platforms is a constant challenge. As noted for sea ice extent, important data sources can be vulnerable to individual satellites reaching the end of their expected lifespan or otherwise failing without adequate replacement. In situ networks are also regularly under pressure, especially in data-sparse regions such as Africa, parts of Asia, and South and Central America. Effective management of the data that are collected, and their transmission through channels from which they can be incorporated into global datasets, are also important.

In parallel with the designation of headline climate indicators, WMO is introducing a framework for the assessment of the maturity of climate datasets incorporating ECVs.[4] A number of dataset providers have submitted their datasets for assessment. This process is still in the early stages of implementation and the fact that a specific dataset has not yet been assessed should not be considered as an indication that it is inferior to those datasets that have been assessed. There is also a need for harmonized standards for data reporting and metadata for balanced assessment of the indicators.

[4] https://climatedata-catalogue.wmo.int/about

Acknowledgments. MDP was supported by the Met Office Hadley Centre Climate Programme funded by BEIS and Defra (United Kingdom). We thank Rachel Killick for providing the EN4 timeseries of ocean heat content change.

References

Abraham, J. P., and Coauthors, 2013: A review of global ocean temperature observations: Implications for ocean heat content estimates and climate change. *Rev. Geophys.*, **51**, 450–483, https://doi.org/10.1002/rog.20022.

Abram, N. J., E. W. Wolff, and M. A. J. Curran, 2013: A review of sea ice proxy information from polar ice cores. *Quat. Sci. Rev.*, **79**, 168–183, https://doi.org/10.1016/j.quascirev.2013.01.011.

Alexander, L. V., M. Bador, R. Roca, S. Contractor, M. G. Donat, and P. L. Nguyen, 2020: Intercomparison of annual precipitation indices and extremes over global land areas from *in situ*, space-based and reanalysis products. *Environ. Res. Lett.*, **15**, 055002, https://doi.org/10.1088/1748-9326/ab79e2.

Allen, M. R., and Coauthors, 2018: Framing and context. *Global Warming of 1.5°C: An IPCC Special Report*, V. Masson-Delmotte et al., Eds., IPCC, 49–91.

Blunden, J., D. S. Arndt, and G. Hartfield, Eds., 2018: State of the Climate in 2017. *Bull. Amer. Meteor. Soc.*, **99** (8), Si–S310, https://doi.org/10.1175/2018BAMSStateoftheClimate.1.

Bojinski, S., M. Verstraete, T. C. Peterson, C. Richter, A. Simmons, and M. Zemp, 2014: The concept of essential climate variables in support of climate research, applications, and policy. *Bull. Amer. Meteor. Soc.*, **95**, 1431–1443, https://doi.org/10.1175/BAMS-D-13-00047.1.

Boyer, T., and Coauthors, 2016: Sensitivity of global upper-ocean heat content estimates to mapping methods, XBT bias corrections, and baseline climatologies. *J. Climate*, **29**, 4817–4842, https://doi.org/10.1175/JCLI-D-15-0801.1.

Braithwaite, R. J., 1981: On glacier energy balance, ablation, and air temperature. *J. Glaciol.*, **27**, 381–391, https://doi.org/10.1017/S0022143000011424.

Braun, M. H., and Coauthors, 2019: Constraining glacier elevation and mass changes in South America. *Nat. Climate Change*, **9**, 130–136, https://doi.org/10.1038/s41558-018-0375-7.

Brun, F., E. Berthier, P. Wagnon, A. Kääb, and D. Treichler, 2017: A spatially resolved estimate of High Mountain Asia glacier mass balances from 2000 to 2016. *Nat. Geosci.*, **10**, 668–673, https://doi.org/10.1038/ngeo2999.

Cazenave, A., and Coauthors, 2019: Observational requirements for long-term monitoring of the global mean sea level and its components over the altimetry era. *Front. Mar. Sci.*, **6**, 582, https://doi.org/10.3389/fmars.2019.00582.

Cheng, L., and Coauthors, 2016: XBT science: Assessment of instrumental biases and errors. *Bull. Amer. Meteor. Soc.*, **97**, 924–933, https://doi.org/10.1175/BAMS-D-15-00031.1.

——, K. E. Trenberth, J. Fasullo, T. Boyer, J. Abraham, and J. Zhu, 2017: Improved estimates of ocean heat content from 1960 to 2015. *Sci. Adv.*, **3**, e1601545, https://doi.org/10.1126/sciadv.1601545.

Comiso, J. C., W. N. Meier, and R. Gersten, 2017: Variability and trends in the Arctic Sea ice cover: Results from different techniques. *J. Geophys. Res. Oceans*, **122**, 6883–6900, https://doi.org/10.1002/2017JC012768.

Cowtan, K., and R. G. Way, 2014: Coverage bias in the HadCRUT4 temperature series and its impact on recent temperature trends. *Quart. J. Roy. Meteor. Soc.*, **140**, 1935–1944, https://doi.org/10.1002/qj.2297.

Davy, R., L. Chen, and E. Hanna, 2018: Arctic amplification metrics. *Int. J. Climatol.*, **38**, 4384–4394, https://doi.org/10.1002/joc.5675.

Desbruyères, D. G., S. G. Purkey, E. L. McDonagh, G. C. Johnson, and B. A. King, 2016: Deep and abyssal ocean warming from 35 years of repeat hydrography. *Geophys. Res. Lett.*, **43**, 10356–10365, https://doi.org/10.1002/2016GL070413.

——, E. L. McDonagh, B. A. King, and V. Thierry, 2017: Global and full-depth ocean temperature trends during the early twenty-first century from Argo and repeat hydrography. *J. Climate*, **30**, 1985–1997, https://doi.org/10.1175/JCLI-D-16-0396.1.

Donat, M. G., L. V. Alexander, H. Yang, I. Durre, R. Vose, and J. Caesar, 2013: Global land-based datasets for monitoring climate extremes. *Bull. Amer. Meteor. Soc.*, **94**, 997–1006, https://doi.org/10.1175/BAMS-D-12-00109.1.

Eisenman, I., W. N. Meier, and J. R. Norris, 2014: A spurious jump in the satellite record: Has Antarctic sea ice expansion been overestimated? *Cryosphere*, **8**, 1289–1296, https://doi.org/10.5194/tc-8-1289-2014.

Etheridge, D. M., L. P. Steele, R. L. Langenfelds, R. J. Francey, J.-M. Barnola, and V. I. Morgan, 1996: Natural and anthropogenic changes in atmospheric CO_2 over the last 1000 years from air in Antarctic ice and firn. *J. Geophys. Res.*, **101**, 4115–4128, https://doi.org/10.1029/95JD03410.

Fetterer, F., K. Knowles, W. N. Meier, M. Savoie, and A. K. Windnagel, 2017: Sea ice index, version 3. National Snow and Ice Data Center, accessed 23 December 2019, https://doi.org/10.7265/N5K072F8.

Freeman, E., and Coauthors, 2017: ICOADS release 3.0: A major update to the historical marine climate record. *Int. J. Climatol.*, **37**, 2211–2232, https://doi.org/10.1002/joc.4775.

Gallaher, D. W., G. G. Campbell, and W. N. Meier, 2014: Anomalous variability in Antarctic sea ice extents during the 1960s with the use of Nimbus data. *IEEE J. Sel. Top. Appl. Earth Obs. Remote Sens.*, **7**, 881–887, https://doi.org/10.1109/JSTARS.2013.2264391.

Gardner, A. S., and Coauthors, 2013: A reconciled estimate of glacier contributions to Sea level rise: 2003 to 2009. *Science*, **340**, 852–857, https://doi.org/10.1126/science.1234532.

Gehne, M., T. M. Hamill, G. N. Kiladis, and K. E. Trenberth, 2016: Comparison of global precipitation estimates across a range of temporal and spatial scales. *J. Climate*, **29**, 7773–7795, https://doi.org/10.1175/JCLI-D-15-0618.1.

Gill, A., 1982: *Atmosphere-Ocean Dynamics.* Academic Press, 662 pp.

Global Climate Observing System, 2017: Indicators of climate change: Outcome of a meeting held at WMO 3 February 2017. GCOS 206, World Meteorological Organization, 29 pp., https://library.wmo.int/doc_num.php?explnum_id=3418.

Good, S. A., M. J. Martin, and N. A. Rayner, 2013: EN4: Quality controlled ocean temperature and salinity profiles and monthly objective analyses with uncertainty estimates. *J. Geophys. Res. Oceans*, **118**, 6704–6716, https://doi.org/10.1002/2013JC009067.

Grove, J. M., 2004: *Little Ice Ages: Ancient and Modern*. Vol. 1. Taylor and Francis, 402 pp.

Gu, G., and R. F. Adler, 2011: Precipitation and temperature variations on the interannual time scale: Assessing the impact of ENSO and volcanic eruptions. *J. Climate*, **24**, 2258–2270, https://doi.org/10.1175/2010JCLI3727.1.

Hawkins, E., and Coauthors, 2017: Estimating changes in global temperature since the preindustrial period. *Bull. Amer. Meteor. Soc.*, **98**, 1841–1856, https://doi.org/10.1175/BAMS-D-16-0007.1.

Herold, N., L. V. Alexander, M. G. Donat, S. Contractor, and A. Becker, 2016: How much does it rain over land? *Geophys. Res. Lett.*, **43**, 341–348, https://doi.org/10.1002/2015GL066615.

Hobbs, W. R., R. Massom, S. Stammerjohn, P. Reid, G. Williams, and W. Meier, 2016: A review of recent changes in Southern Ocean sea ice, their drivers and forcings. *Global Planet. Change*, **143**, 228–250, https://doi.org/10.1016/j.gloplacha.2016.06.008.

Horwath, M., and Coauthors, 2020: ESA Climate Change Initiative (CCI) Sea Level Budget Closure (SLBC_cci) final report D4.7, version 1.1. European Space Agency, 101 pp, https://climate.esa.int/media/documents/ESA_SLBC_cci_D4.7_v1.1.pdf.

Huffman, G. J., R. F. Adler, D. T. Bolvin, and G. Gu, 2009: Improving the global precipitation record: GPCP version 2.1. *Geophys. Res. Lett.*, **36**, L17808, https://doi.org/10.1029/2009GL040000.

IPCC, 2013: *Climate Change 2013: The Physical Science Basis*. Cambridge University Press, 1585 pp.

——, 2019a: *IPCC Special Report on the Ocean and Cryosphere in a Changing Climate*. H.-O. Pörtner et al., Eds., IPCC, 755 pp., https://www.ipcc.ch/srocc/download/.

——, 2019b: *Climate Change and Land: An IPCC Special Report on Climate Change, Desertification, Land Degradation, Sustainable Land Management, Food Security, and Greenhouse Gas Fluxes in Terrestrial Ecosystems.* P. R. Shukla et al., Eds., IPCC, 864 pp., https://www.ipcc.ch/site/assets/uploads/2019/11/SRCCL-Full-Report-Compiled-191128.pdf.

Ivanova, N., and Coauthors, 2015: Inter-comparison and evaluation of sea ice algorithms: Towards further identification of challenges and optimal approach using passive microwave observations. *Cryosphere*, **9**, 1797–1817, https://doi.org/10.5194/tc-9-1797-2015.

Johnson, G. C., and Coauthors, 2019: Ocean heat content [in "State of the Climate in 2018"]. *Bull. Amer. Meteor. Soc.*, **100** (9), S74–S77, https://doi.org/10.1175/2019BAMSStateoftheClimate.1.

Kääb, A., E. Berthier, C. Nuth, J. Gardelle, and Y. Arnaud, 2012: Contrasting patterns of early twenty-first-century glacier mass change in the Himalayas. *Nature*, **488**, 495–498, https://doi.org/10.1038/nature11324.

Kennedy, J. J., N. A. Rayner, C. P. Atkinson, and R. E. Killick, 2019: An ensemble data set of sea surface temperature change from 1850: The Met Office Hadley Centre HadSST.4.0.0.0 data set. *J. Geophys. Res. Atmos.*, **124**, 7719–7763, https://doi.org/10.1029/2018JD029867.

King, A. D., M. G. Donat, and R. J. H. Dunn, 2019: Land surface temperature extremes [in "State of the Climate in 2018"]. *Bull. Amer. Meteor. Soc.*, **100** (9), S14–S16, https://doi.org/10.1175/2019BAMSStateoftheClimate.1.

Kinnard, C., C. M. Zdanowicz, D. A. Fisher, E. Isaksson, A. de Vernal, and L. G. Thompson, 2011: Reconstructed changes in Arctic sea ice over the past 1,450 years. *Nature*, **479**, 509–512, https://doi.org/10.1038/nature10581.

Lavergne, T., and Coauthors, 2019: Version 2 of the EUMETSAT OSI SAF and ESA CCI sea-ice concentration climate data records. *Cryosphere*, **13**, 49–78, https://doi.org/10.5194/tc-13-49-2019.

Leclercq, P. W., J. Oerlemans, H. J. Basagic, I. Bushueva, A. J. Cook, and R. Le Bris, 2014: A data set of worldwide glacier length fluctuations. *Cryosphere*, **8**, 659–672, https://doi.org/10.5194/tc-8-659-2014.

Legeais, J. F., and Coauthors, 2018: An improved and homogeneous altimeter sea level record from the ESA Climate Change Initiative. *Earth Syst. Sci. Data*, **10**, 281–301, https://doi.org/10.5194/essd-10-281-2018.

Lyman, J. M., and G. C. Johnson, 2008: Estimating annual global upper-ocean heat content anomalies despite irregular in situ ocean sampling. *J. Climate*, **21**, 5629–5641, https://doi.org/10.1175/2008JCLI2259.1.

Marcott, S. A., and Coauthors, 2014: Centennial-scale changes in the global carbon cycle during the last deglaciation. *Nature*, **514**, 616–619, https://doi.org/10.1038/nature13799.

Marzeion, B., J. G. Cogley, K. Richter, and D. Parkes, 2014: Attribution of global glacier mass loss to anthropogenic and natural causes. *Science*, **345**, 919–921, https://doi.org/10.1126/science.1254702.

Meier, W. N., and J. J. Stewart, 2019: Assessing uncertainties in sea ice extent climate indicators. *Environ. Res. Lett.*, **14**, 035005, https://doi.org/10.1088/1748-9326/aaf52c.

Meyssignac, B., and Coauthors, 2019: Measuring global ocean heat content to estimate the earth energy imbalance. *Front. Mar. Sci.*, **6**, 432, https://doi.org/10.3389/fmars.2019.00432.

Morice, C. P., J. J. Kennedy, N. A. Rayner, and P. D. Jones, 2012: Quantifying uncertainties in global and regional temperature change using an ensemble

of observational estimates: The HadCRUT4 data set. *J. Geophys. Res.*, **117**, D08101, https://doi.org/10.1029/2011JD017187.

Nerem, R. S., B. D. Beckley, J. Fasullo, B. D. Hamlington, D. Masters, and G. T. Mitchum, 2018: Climate change driven accelerated sea level rise detected in the altimeter era. *Proc. Natl. Acad. Sci. USA*, **115**, 2022–2025, https://doi.org/10.1073/pnas.1717312115.

Ohmura, A., 2001: Physical basis for the temperature-based melt-index method. *J. Appl. Meteor.*, **40**, 753–761, https://doi.org/10.1175/1520-0450(2001)040<0753:PBFTTB>2.0.CO;2.

Palmer, M. D., 2017: Reconciling estimates of ocean heating and Earth's radiation budget. *Curr. Climate Change Rep.*, **3**, 78–86, https://doi.org/10.1007/s40641-016-0053-7.

——, and P. Brohan, 2011: Estimating sampling uncertainty in fixed-depth and fixed-isotherm estimates of ocean warming. *Int. J. Climatol.*, **31**, 980–986, https://doi.org/10.1002/joc.2224.

——, and D. J. McNeall, 2014: Internal variability of Earth's energy budget simulated by CMIP5 climate models. *Environ. Res. Lett.*, **9**, 034016, https://doi.org/10.1088/1748-9326/9/3/034016.

——, K. Haines, S. F. B. Tett, and T. J. Ansell, 2007: Isolating the signal of ocean global warming. *Geophys. Res. Lett.*, **34**, L23610, https://doi.org/10.1029/2007GL031712.

——, and Coauthors, 2017: Ocean heat content variability and change in an ensemble of ocean reanalyses. *Climate Dyn.*, **49**, 909–930, https://doi.org/10.1007/s00382-015-2801-0.

Parkinson, C. L., 2019: A 40-y record reveals gradual Antarctic sea ice increases followed by decreases at rates far exceeding the rates seen in the Arctic. *Proc. Natl. Acad. Sci. USA*, **116**, 14414–14423, https://doi.org/10.1073/pnas.1906556116.

Perkins-Kirkpatrick, S. E., M. G. Donat, and R. J. H. Dunn, 2018: Land surface temperature extremes [in "State of the Climate in 2017"]. *Bull. Amer. Meteor. Soc.*, **99** (8), S15–S16, https://doi.org/10.1175/2018BAMSStateoftheClimate.1.

Peterson, T. C., and M. J. Manton, 2008: Monitoring changes in climate extremes: A tale of international cooperation. *Bull. Amer. Meteor. Soc.*, **89**, 1266–1271, https://doi.org/10.1175/2008BAMS2501.1.

Pfeffer, W. T., and Coauthors, 2014: The Randolph glacier inventory: A globally complete inventory of glaciers. *J. Glaciol.*, **60**, 537–552, https://doi.org/10.3189/2014JoG13J176.

Purkey, S. G., and G. C. Johnson, 2010: Warming of global abyssal and deep southern ocean waters between the 1990s and 2000s: Contributions to global heat and sea level rise budgets. *J. Climate*, **23**, 6336–6351, https://doi.org/10.1175/2010JCLI3682.1.

Riser, S. C., and Coauthors, 2016: Fifteen years of ocean observations with the global Argo array. *Nat. Climate Change*, **6**, 145–153, https://doi.org/10.1038/nclimate2872.

Roemmich, D., W. J. Gould, and J. Gilson, 2012: 135 years of global ocean warming between the Challenger expedition and the Argo Programme. *Nat. Climate Change*, **2**, 425–428, https://doi.org/10.1038/nclimate1461.

Simmons, A. J., P. Berrisford, D. P. Dee, H. Hersbach, S. Hirahara, and J.-N. Thépaul, 2017: A reassessment of temperature variations and trends from global reanalyses and monthly surface climatological datasets. *Quart. J. Roy. Meteor. Soc.*, **143**, 101–119, https://doi.org/10.1002/qj.2949.

Tye, M. R., S. Blenkinsop, M. Donat, I. Durre, and M. Ziese, 2018: Land surface precipitation extremes [in "State of the Climate in 2017"]. *Bull. Amer. Meteor. Soc.*, **99** (8), S29–S31, https://doi.org/10.1175/2018BAMSStateoftheClimate.1.

United Nations, 2015a: Paris Agreement. United Nations, 27 pp., https://unfccc.int/files/essential_background/convention/application/pdf/english_paris_agreement.pdf.

——, 2015b: Transforming our world: The 2030 agenda for sustainable development. United Nations, 44 pp., https://sustainabledevelopment.un.org/post2015/transformingourworld/publication.

von Schuckmann, K., and Coauthors, 2016: An imperative to monitor Earth's energy imbalance. *Nat. Climate Change*, **6**, 138–144, https://doi.org/10.1038/nclimate2876.

——, and Coauthors, 2018: Copernicus marine service ocean state report. *J. Oper. Oceanogr.*, **11** (Suppl. 1), S1–S142, https://doi.org/10.1080/1755876X.2018.1489208.

Vose, R. S., R. Adler, A. Becker, and X. Yin, 2018: Precipitation [in "State of the Climate in 2017"]. *Bull. Amer. Meteor. Soc.*, **99** (8), S28–S31, https://doi.org/10.1175/2018BAMSStateoftheClimate.1.

Walsh, J. E., F. Fetterer, J. S. Stewart, and W. L. Chapman, 2017: A database for depicting Arctic sea ice variations back to 1850. *Geogr. Rev.*, **107**, 89–107, https://doi.org/10.1111/j.1931-0846.2016.12195.x.

Wijffels, S. E., D. Roemmich, D. Monselesan, J. Church, and J. Gilson, 2016: Ocean temperatures chronicle the ongoing warming of Earth. *Nat. Climate Change*, **6**, 116–118, https://doi.org/10.1038/nclimate2924.

Williams, M., and S. Eggleston, 2017: Using indicators to explain our changing climate to policymakers and the public. *WMO Bull.*, **66**, 33–39.

Witze, A., 2017: Ageing satellites put crucial sea-ice climate record at risk. *Nature*, **551**, 13–14, https://doi.org/10.1038/nature.2017.22907.

Wong, A., R. Keeley, and T. Carval, 2018: Argo quality control manual for CTD and trajectory data. Ifremer, accessed 15 April 2020, https://doi.org/10.13155/33951.

WCRP Global Sea Level Budget Group, 2018: Global sea-level budget 1993-present. *Earth Syst. Sci. Data*, **10**, 1551–1590, https://doi.org/10.5194/essd-10-1551-2018.

WMO, 2009: Technical Report of Global Analysis Method for Major Greenhouse Gases by the World Data Center for Greenhouse Gases. GAW Rep. 184, WMO/TD-1473, World Meteorological Organization, 31 pp., www.wmo.int/pages/prog/arep/gaw/documents/TD_1473_GAW184_web.pdf.

——, 2015: *Status of the Global Observing System for Climate.* World Meteorological Organization, 373 pp.

——, 2017a: Expert meeting on the WMO Statements on the Status of the Global Climate: Meeting report. WCDMP-84, World Meteorological Organization, 18 pp., www.wmo.int/pages/prog/wcp/wcdmp/documents/Report-Expert-meeting_final-WCDMP-84.pdf.

——, 2017b: WMO guidelines on the calculation of climate normals. WMO-1203, World Meteorological Organization, 29 pp., https://library.wmo.int/doc_num.php?explnum_id=4166.

——, 2018a: Commission for Climatology: A bridged final report of the Seventeenth Session. WMO-1216, World Meteorological Organization, 57 pp., https://library.wmo.int/doc_num.php?explnum_id=4611.

——, 2018b: 19th WMO/IAEA Meeting on Carbon Dioxide, Other Greenhouse Gases and Related Measurement Techniques (GGMT-2017). GAW Tech. Rep. 242, World Meteorological Organization, 134 pp., https://library.wmo.int/doc_num.php?explnum_id=5456.

——, 2018c: WMO statement on the state of the global climate in 2017. WMO-1212, World Meteorological Organization, 35 pp., https://library.wmo.int/doc_num.php?explnum_id=4453.

——, 2019: WMO statement on the state of the global climate in 2018. WMO-1233, World Meteorological Organization, 39 pp., https://library.wmo.int/doc_num.php?explnum_id=5789.

Wouters, B., A. S. Gardner, and G. Moholdt, 2019: Global glacier mass loss during the GRACE satellite mission (2002-2016). *Front. Earth Sci.*, **7**, 96, https://doi.org/10.3389/feart.2019.00096.

Zanna, L., S. Khatiwala, J. M. Gregory, J. Ison, and P. Heimbach, 2019: Global reconstruction of historical ocean heat storage and transport. *Proc. Natl. Acad. Sci. USA*, **116**, 1126–1131, https://doi.org/10.1073/pnas.1808838115.

Zemp, M., and Coauthors, 2015: Historically unprecedented global glacier decline in the early 21st century. *J. Glaciol.*, **61**, 745–762, https://doi.org/10.3189/2015JoG15J017.

——, and Coauthors, 2019: Global glacier mass changes and their contributions to sea-level rise from 1961 to 2016. *Nature*, **568**, 382–386, https://doi.org/10.1038/s41586-019-1071-0.